| | |
|---|---|
| Title | Effect of Fabricating Process on Notch Toughness of Shipbuilding Steel Plates (Report I) : Effect of Line-Heating on Notch Toughness of 50 kg/mm^2-Class High-Tensile Steel Plates |
| Author(s) | Kihara, Hiroshi; Suhara, Jiro; Kurokawa, Tsuneo et al. |
| Citation | Transactions of JWRI. 1974, 3(2), p. 167-184 |
| Version Type | VoR |
| URL | https://doi.org/10.18910/8844 |
| rights | |
| Note | |

# Effect of Fabricating Process on Notch Toughness of Shipbuilding Steel Plates (Report I)†
## —Effect of Line-Heating on Notch Toughness of 50 kg/mm²-Class High-Tensile Steel Plates—


Hiroshi KIHARA*, Jiro SUHARA**, Tsuneo KUROKAWA***, Shigeo KATAOKA****,
Masaki NAKAJIMA***** and Hiroshi YAJIMA******



**Abstract**

*Local embrittlement of the surface layer of line-heated steel plates may not be deep enough to warrant the rejection when carefully analyzed having due regards to the ratio of the heat-affected layer to the full plate thickness. The authors carried out V-notch Charpy impact test, brittle fracture initiation test, and brittle fracture propagation arrest test on 50 kg/mm² high-tensile plate specimens to evaluate the effect of line-heating on their notch toughness for the full plate thickness. It was found that the effect of line-heating would vary with the water- and air-cooling, and, especially, with the manner in which the water-cooling was provided, and that by choosing proper medium and timing for cooling, the steel plates could be line-heated more efficiently without adverse effects on their notch toughness.*


### 1. Introduction

Line-heating[1] is the thermoplastic working of metals and is widely applied in bending and straightening of shipbuilding steel plates. When used on the mild steel plates, it usually consists of heating with the torch flame to above the transformation temperature $Ac_1$ and rapid cooling with water. For the 50 kg/mm² -class high-tensile steel plates with some hardenability, however, is said that the flame heating should be limited to below the transformation temperature and also rapid water-cooling should be avoided so as not to impair mechanical properties, especially notch toughness, of the steel plates though under what conditions to apply the line-heating is not clearly made known.

Line-heating on the steel plate does lead to local embrittlement of the plate surface The line-heated steel plate, when Charpy-tested at the heated zone, will naturally show low impact values which are unacceptable to the classification societies. Actually, however, such local embrittlement may not be deep enough to warrant the rejection when carefully analyzed having due regards to the ratio of the heat-affected layer to the full thickness of the steel plate. Thus, propriety of the generally accepted practice of evaluating the brittle fracture strength of the line-heated steel plate merely by testing the heated zone for notch toughness is to be challenged.

In view of the above, the authors carried out V-notch Charpy impact test, brittle fracture initiation test, and brittle fracture propagation arrest test on line-heated-and-notched 50 kg/mm² high-tensile wide-plate test specimens to quantitatively determine the relations between the line-heating conditions, Charpy impact values, brittle fracture initiation in the heated zone, and resistance to brittle fracture propagation, for the full plate thickness.

### 2. Principle of Thermoplastic Metalworking by Line-Heating

When line-heated, a steel plate undergoes angular distortions as illustrated in **Figs. 1 (a), (b),** and **(c).** Heated by the torch flame linearly as shown in (a), the steel plate first becomes distorted as shown in (b) and, when water-cooled, distorted backwards as shown in (c). More specifically, when the plate


† Received on Jan. 10, 1974


* Previously Director and Emeritus Professor
** Professor, Kyushu University
*** Professor, Nagasaki University
**** Research Assistant, Nagasaki University
***** Manager, Welding Research Laboratory, Nagasaki Technical Institute, Mitsubishi Heavy Industries, Ltd.
****** Senior Research Engineer, Nagasaki Technical Institute, Mitsubishi Heavy Industries, Ltd.

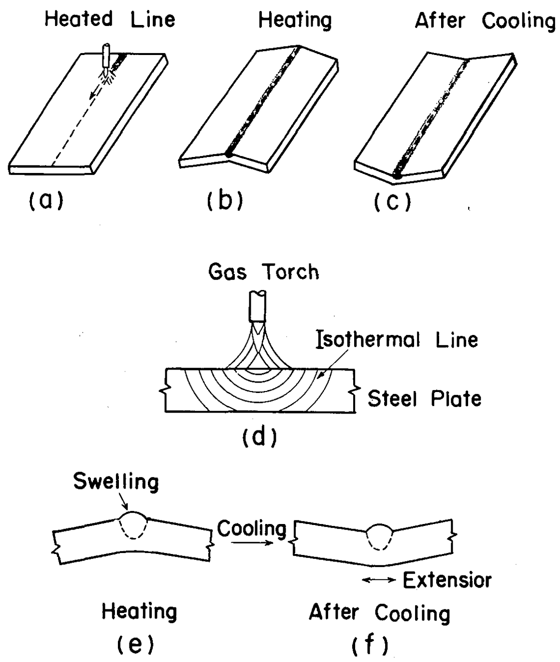


Fig. 1. Thermoplastic working by line-heating.

surface is heated by the torch flame linearly as shown in (a), the temperature gradient is produced across the plate thickness as shown in **(d)** and the plate undergoes angular distortion as shown in (b) since the plate expands more at the heated side than it does at the opposite side: the lower temperature at the opposite side than gives rise to the elastic reaction to resist the angular distortion and, as a result, the plate partially yields at the heated side and produces a swell as shown in **(e)**: when water-cooled the plate contracts at the heated side except for the swollen part and therefore becomes distorted backwards as shown in **(f)**.

## 3. High-Tensile Steels Used in Tests

Test specimens were prepared from 30 mm thick Grade A (K5A), 30 mm and 12.7 mm thick Grade D (K5D), and 30 mm thick Grade E (K5E) 50 kg/mm$^2$ high-tensile steel plates manufactured to the rules and regulations of Nippon Kaiji Kyokai (the ship classification society of Japan). Chemical compositions and mechanical properties of the steel plates are shown in **Table 1.** Also, a round tensile test specimen 6 mm in diameter and 24 mm in gauge length was cut from the mid-thickness of each steel plate, and by tension test the relation between yield stress and temperature in the 0∼−196°C temperature range was determined as follows.

K5A steel plate (30 mm thick): $\sigma_y = 25.5e^{95.0/T_K}$ ---------(1)

K5D steel plate (30 mm thick): $\sigma_y = 31.8e^{83.9/T_K}$ ---------(2)

K5E steel plate (30 mm thick): $\sigma_y = 31.8e^{83.9/T_K}$ ---------(3)

K5D steel plate (12.7 mm thick): $\sigma_y = 28.4e^{83.9/T_K}$ --------(4)

where $\sigma_y$ = yield stress, kg/mm$^2$

$T_K$ = absolute temperature, °K

## 4. Methods of Line-Heating

Two different methods of line-heating are in general use; the straight line-heating in which the torch is moved linearly and the weaving line-heating in which the torch is moved describing many small circles. The test specimens were all line-heated linearly, and **Table 2** shows the line-heating conditions adopted. As illustrated below the table, a carriage having in tandem an oxy-acetylene torch and a cooling-water nozzle was used. **Figure 2** shows the relation between torch travel speed and maximum heating temperature. For measurement of the heating temperature, a 1.5 mm diam. hole was drilled from the back of the plate until it was 1 mm short of reaching the heated surface and a 0.3 mm diam. CA thermocouple was percussion-welded to the bottom of the drilled hole and connected to an electromagnetic oscillograph at the outside. The maximum heating temperature measured is, therefore, the highest temperature reading in thermal cycle in the plate 1 mm below the heated surface, which means that the actual heating temperature at the exposed plate surface must have been considerably higher.

For test purposes, the water-cooling was provided in different manners: the water-cooling immediately after heating, by placing the torch and cooling-water

Table 1. Chemical compositions and mechanical properties of steels used.

| Specification | Heat Treatment | Plate Thickness (mm) | Chemical Compositions (%) | | | | | Tensile Properties | | |
|---|---|---|---|---|---|---|---|---|---|---|
| | | | C | Si | Mn | P | S | Y. P. (kg/mm$^2$) | T. S. (kg/mm$^2$) | Elong. (%) (G. L.=200 mm) |
| K5A | As Rolled | 30 | 0.12 | 0.34 | 1.24 | 0.025 | 0.020 | 37.8 | 52.4 | 25.2 |
| K5D | Normalized | 30 | 0.15 | 0.46 | 1.31 | 0.014 | 0.019 | 36.0 | 53.0 | 24.0 |
| K5E | Normalized | 30 | 0.13 | 0.35 | 1.35 | 0.027 | 0.017 | 38.2 | 55.1 | 23.7 |
| K5D | As Rolled | 12.7 | 0.15 | 0.46 | 1.31 | 0.014 | 0.019 | 39.0 | 55.0 | 23.0 |

Table 2. Conditions of line-heating.

| Item | Condition |
|---|---|
| Nozzle of Gas Torch | 2.8 mm$^{\phi}$ |
| Pressure of Oxygen | 6.0 kg/cm$^2$ |
| Flow Rate of Oxygen | $2.3 \times 10^3$ ℓ/h |
| Pressure of Acetylene | 0.5 kg/cm$^2$ |
| Flow Rate of Acetylene | $2.0 \times 10^3$ ℓ/h |
| Height of Gas Torch (H) | 20 mm |
| Distance between Gas Torch and Water Nozzle (D) | Min. 50 mm |
| Flow Rate of Water | 2.3 ℓ/min |

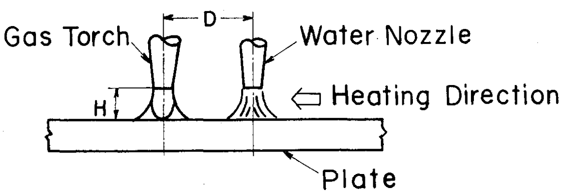


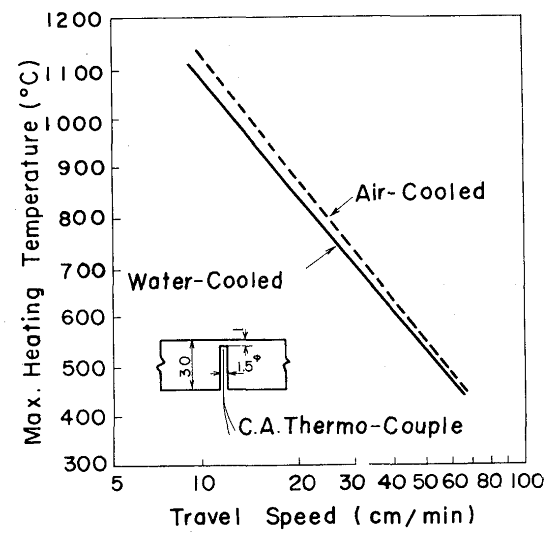


Fig. 2. Relationship between travel speed of torch and maximum heating temperature.

nozzle at the minimum of 50 mm distances; and the water-cooling with increasingly longer time delay after heating, by placing the torch and cooling-water nozzle at increasingly greater distances and thus allowing the heated plate surface to cool in air accordingly before water-cooled. **Figure 3** shows an example of the thermal cycle for the plate which was line-heated to the maximum of 800°C and water-cooled immediately afterwards. It will be seen from the figure that though the plate was water-cooled immediately after heating, its temperature decreased by 100°C to about 700°C before the water-cooling was started. For reference,

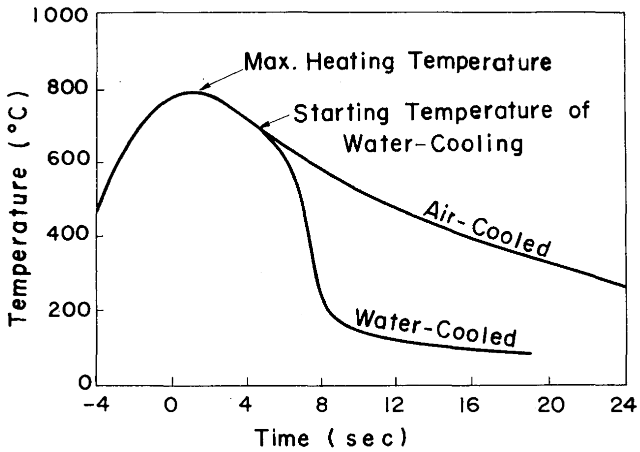


Fig. 3. Example of thermal cycle of line-heated zone (1 mm below the heated surface).

temperature distributions on the plate surface and across the plate thickness at the maximum heating temperature of 800°C are shown in **Figs. 4** and **5**, in which the symbol "800°C $\xrightarrow{A.C.}$ 700°C W.C." indicates that the plate surface was heated to the maximum of 800°C and cooled in air to 700°C before the water-cooling was started.

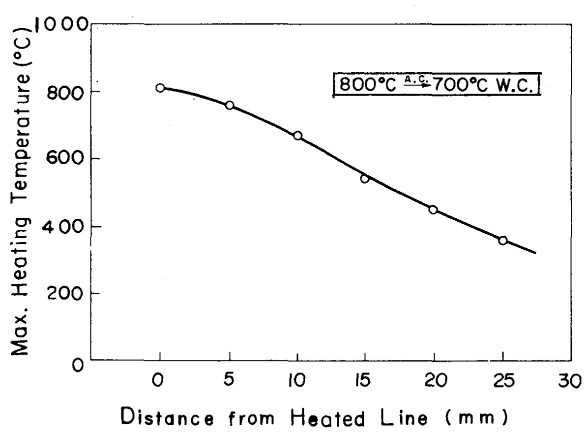


Fig. 4. Example of distribution of maximum heating temperature attained on plate surface (1 mm below the heated surface).

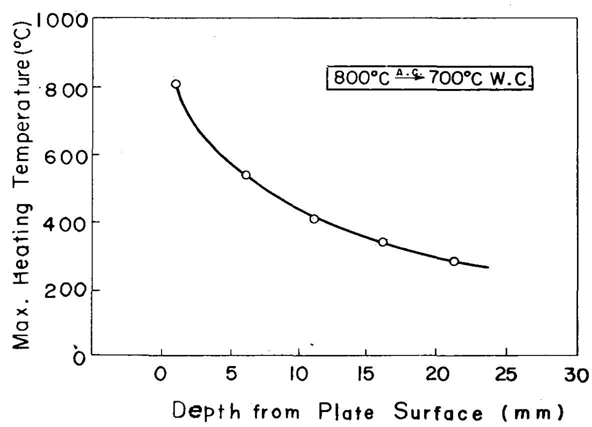


Fig. 5. Example of distribution of maximum heating temperature attained at plate section.

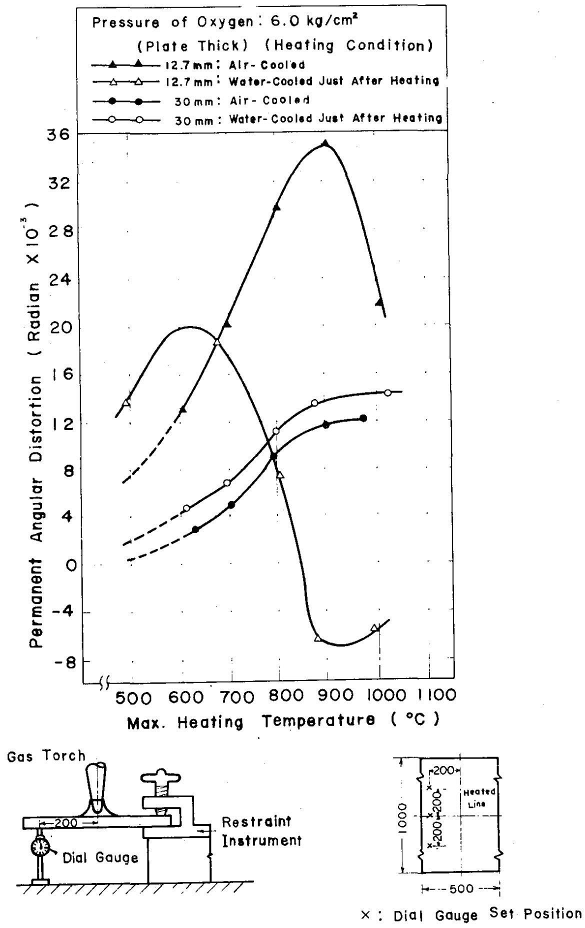


Fig. 6. Relationship between maximum heating temperature and permanent angular distortion.

To see how the angular distortion of the line-heated steel plate would vary with the water- and air-cooling methods, 30 mm and 12.7 mm thick K5D high-tensile test specimens were line-heated and cooled with water or in air. **Figure 6** shows for these specimens the relation between the maximum heating temperature and the permanent angular distortion, and also the method used for measurement of distortion. It will be seen from the figure that for the 30mm thick specimen, the higher the heating temperature, the greater becomes the angular distortion whether the specimen is water- or air-cooled after heating, and that at the maximum heating temperatures in excess of about 900°C, the rate of increase in angular distortion becomes small when the specimen is air-cooled while it becomes great when the specimen is water-cooled. Also, it will be seen that for the 12.7 mm thick specimen, the angular distortion is greatest when air-cooled after heating to about 900°C and when water-cooled after heating to about 600°C. It may be mentioned in this connection that the 12.7 mm thick specimen showed a tendency for the reverse angular distortion when water-cooled after being heated to above 850°C.

## 5. Test Methods

The line-heated steel plates generally are Charpy-tested for notch toughness at the heated zone. The authors line-heated the wide-plate test specimens to different temperatures and cooled them with water or in air, for test by Charpy V-notch impact method. The authors then evaluated the effects of line-heating on the notch toughness for the full plate thickness by conducting brittle fracture initiation and brittle fracture propagation arrest tests on the specimens under typical service conditions. The deep-notch test[2] was used to determine the brittle fracture initiation characteristics and the double-tension[3] or ESSO[4] test to determine the characteristics of brittle fracture propagation arrest.

## 6. Test Specimens

### 6.1 Specimens for V-Notch Charpy Impact Test

250 mm wide (in the direction of roll) $\times$ 600 mm long test plates were prepared from each of the four different steel plates, given one pass of line-heating respectively to different temperatures longitudinally from one side, water- or air-cooled, and skimmed 1 mm of plate thickness by machining throughout the full length of the heated line. Then, a Charpy impact test specimen was taken from each line-heated plate with its axis at right angles to the heated line V-notched perpendicular to the plate surface at the center of the heated zone.

### 6.2 Specimens for Brittle Fracture Initiation Test

400 mm wide $\times$ 500 mm long standard test specimens were prepared from each of the four different steel plates, given one pass of line-heating respectively to different temperatures transversely from each side, water- or air-cooled, and notched with a 120 mm long saw cut from each of two plate edges inwards along the center of the heated line, as shown in **Fig. 7.**

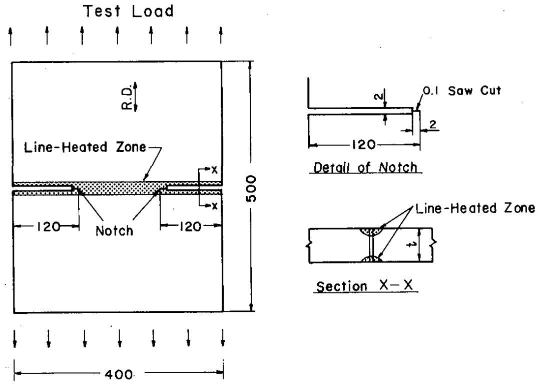


Fig. 7. Deep-notch test specimen.

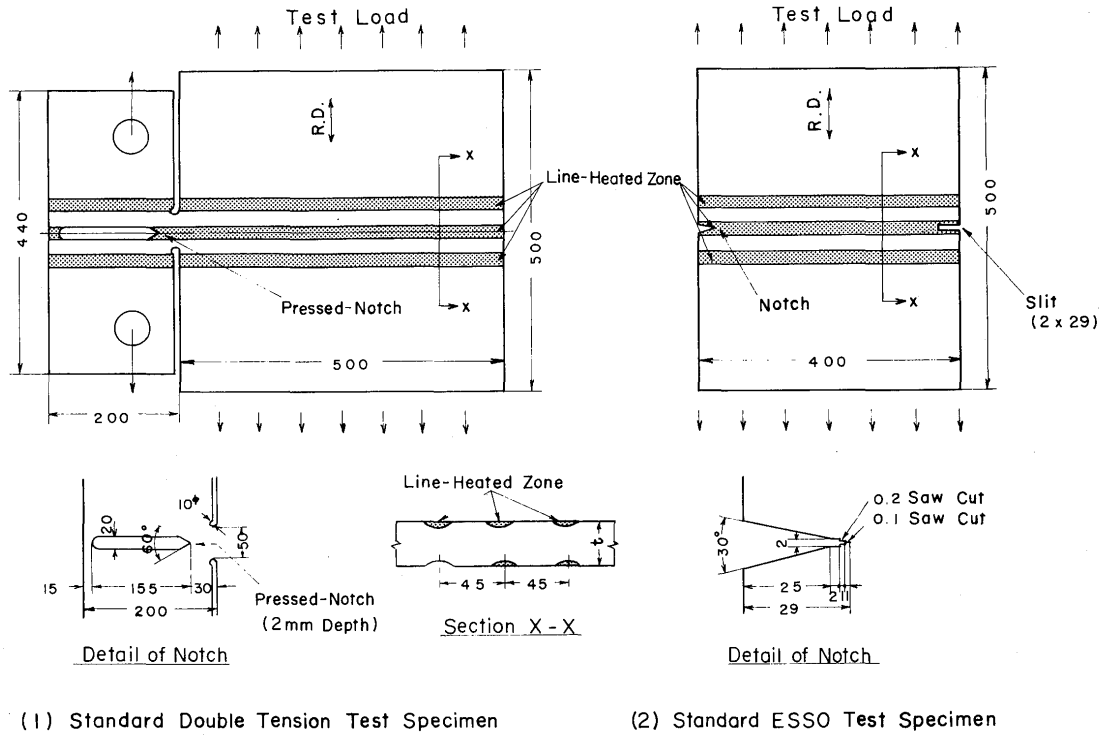


Fig. 8. Double-tension test and ESSO test specimens.

### 6.3 Specimens for Brittle Fracture Propagation Arrest Test

It is generally known that the standard temperature-gradient method of double-tension test on a 500 mm wide press-notched specimen and the standard temperature-gradient method of ESSO test on a 400 mm wide edge-notched specimen will give the same test results. See **Figs. 8 (1)** and **(2)** for details of the specimens. These two types of specimen were prepared from each of the four different steel plates, given one pass each of three full-length line-heatings transversely from each side with a 45 mm distance between the heated lines, and water- or air-cooled, as indicated. Notches were provided so as to let the crack propagate in the center heated line, with the two adjoining heated lines serving to balance the residual stress in the plate and thereby confine the crack propagation to within the center heated line.

## 7. Test Results

### 7.1 V-Notch Carpy Impact Test

**Figures 9~14** shows examples of crystallinity-temperature and energy-temperature curves drawn from the Charpy-test results: Figs. 9~12 show the curves for the specimens line-heated to 800°C or 900°C and water-cooled from different temperatures; Fig. 13 shows the curves for the specimens line-heated to 800°C, 900°C, or 1000°C and air-cooled afterwards while Fig. 14 the curves for the specimens line-heated to 650°C, 700°C, 750°C, 800°C, or 900°C and water-cooled from different temperatures. From these curves, the relation between the 50 % crystallinity transition temperature ${}_vT_{rs}$ and the water- or air-cooling starting temperature was determined for the K5A, K5D, and K5E plate specimens line-heated to 800°C or 900°C, as shown in **Fig. 15.**

From the results of the Charpy-test, the following can be said.

(1) For all the specimens taken from the four different steel plates, the 50 % crystallinity transition temperature ${}_vT_{rs}$ varies considerably with the cooling method adopted though the manner in which ${}_vT_{rs}$ varies is dependent upon the steel grade.
(2) When line-heated to 700°C and air-cooled, all the specimens taken from the K5D and K5E steel plates hardly show any sign of embrittlement.
(3) For the specimens taken from K5A and K5D steel plates, ${}_vT_{rs}$ shifts about 10°C to the high-temperature region when line-heated to 800~900°C and air-cooled while ${}_vT_{rs}$ shifts similarly more than 20°C for the specimens taken from K5E steel plate.
(4) For the specimens taken from K5D steel plate, ${}_vT_{rs}$ shifts about 10°C to the high-temperature region when line-heated to below the transformation temperature $Ac_1$ and water-cooled immediately afterwards (650°C $\xrightarrow{A.C.}$ 575°C W.C.).
(5) For the specimens taken from K5A steel plate,

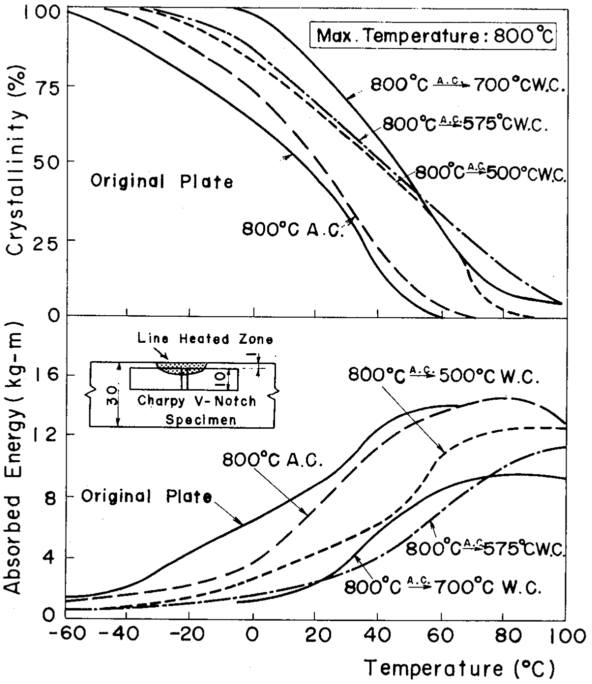


Fig. 9. Charpy V-notch transition curves of line-heated zones, heated to 800°C and water-cooled from various temperatures on cooling cycle (K5A).

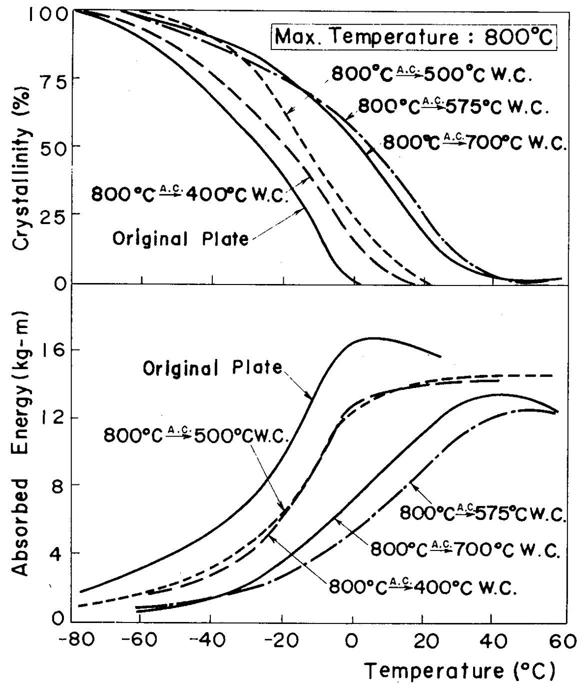


Fig. 10. Charpy V-notch transition curves of line-heated zones, heated to 800°C and water-cooled from various temperatures on cooling cycle (K5D).

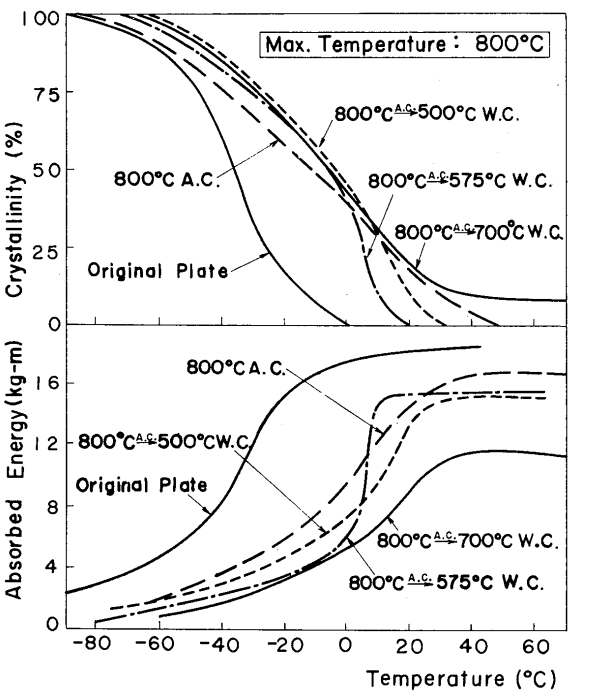


Fig. 11. Charpy V-notch transition curves of line-heated zones, heated to 800°C and water-cooled from various temperatures on cooling cycle (K5E).

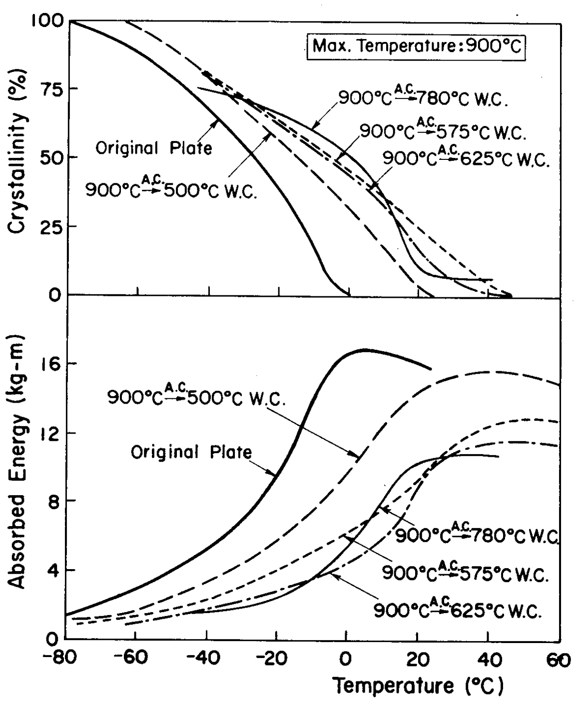


Fig. 12. Charpy V-notch transition curves of line-heated zones, heated to 900°C and water-cooled from various temperatures on cooling cycle (K5D).

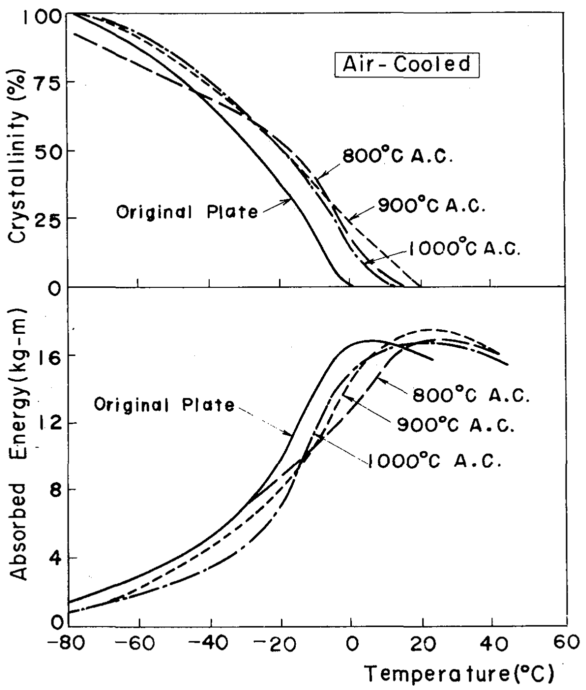


Fig. 13. Charpy V-notch transition curves of line-heated zones, heated to various maximum temperatures and air-cooled (K5D).

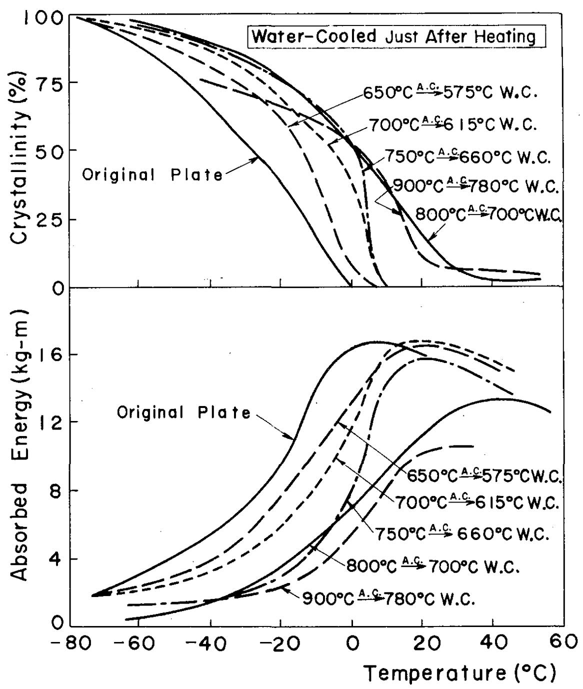


Fig. 14. Charpy V-notch transition curves of line-heated zones, heated to various maximum temperatures and water-cooled just after heating (K5D).

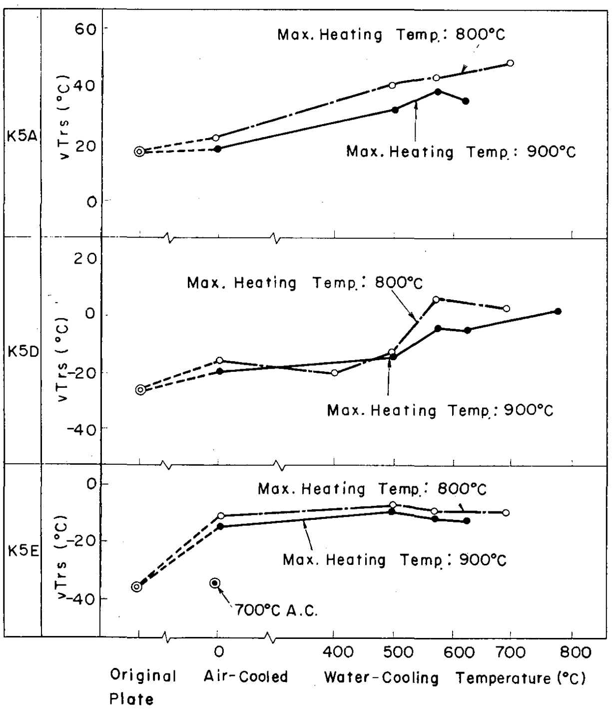


Fig. 15. Effect of water-cooling temperature on Charpy V-notch transition temperature $_vT_{rs}$ of line-heated zone.

$_vT_{rs}$ shifts about 15~30°C to the high-temperature region in all instances when line-heated to 700°C (near the transformation temperature) or to 800~900°C (above the transformation temperature) and water-cooled even though the water-cooling is started from different temperatures: For the specimens taken from K5D steel plate, $_vT_{rs}$ sifts about 10°C and 20~30°C to the high-temperature region when line-heated to 800°C and water-cooled from 500°C and 575°C, respectively: For the specimens taken from K5E steel plate, $_vT_{rs}$ shifts invariably about 20~30°C to the high-temperature region regardless of from what temperature the water-cooling is started.

### 7.2 Brittle Fracture Initiation Test

**Figures 16~19** show the results of brittle fracture initiation tests on the specimens prepared as described in 6.2. The critical plastic surface energy $S_i$, which gives rise to the brittle fracture initiation, was calculated by the following equations.

$$S_i = \frac{\pi[f(\gamma')\cdot \sigma_g]^2 C}{2E} \qquad (5)$$

where $$f(\gamma') = \sqrt{\frac{2}{\pi\gamma'}}\left(\tan\frac{\pi\gamma'}{2} + 0.1\,\mathrm{Sin}\,\pi\gamma'\right) \qquad (6)$$

$$\gamma' = \frac{C}{B} \qquad (7)$$

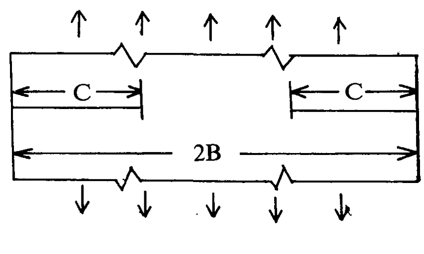

| Spec. | No. | Symbol | Line-Heat Condition | Empirical Formula |
|---|---|---|---|---|
| K5A | ① | ▲ | Original Plate | $Si=100.0\cdot e^{\frac{-610.8}{T_K}}$ |
| | ② | △ | 800°C $\xrightarrow{A.C.}$ 700°C W.C. | $Si=25.0\cdot e^{\frac{-610.8}{T_K}}$ |
| | ③ | ◬ | 800°C $\xrightarrow{A.C.}$ 500°C W.C. | $Si=42.0\cdot e^{\frac{-610.8}{T_K}}$ |
| | ④ | ◬ | 800°C A.C. | $Si=56.7\cdot e^{\frac{-610.8}{T_K}}$ |

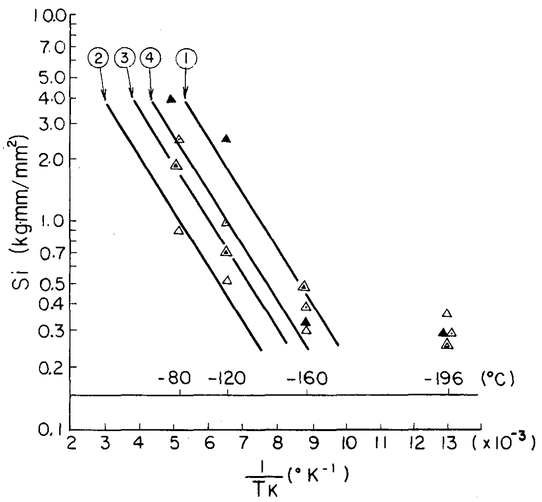


Fig. 16. Results of brittle crack initiation test (Deep-notch test, K5A, thickness; 30 mm).

| Spec. | No. | Symbol | Line-Heat Condition | Empirical Formula |
|---|---|---|---|---|
| K5E | ① | ● | Original Plate | $Si=268.0\cdot e^{\frac{-610.8}{T_K}}$ |
| | ② | ◯ (bold) | 900°C $\xrightarrow{A.C.}$ 500°C W.C. | $Si=119.0\cdot e^{\frac{-610.8}{T_K}}$ |
| | ③ | ○ | 800°C $\xrightarrow{A.C.}$ 700°C W.C. | $Si=35.1\cdot e^{\frac{-610.8}{T_K}}$ |
| | ④ | ◎ | 800°C $\xrightarrow{A.C.}$ 500°C W.C. | $Si=119.0\cdot e^{\frac{-610.8}{T_K}}$ |

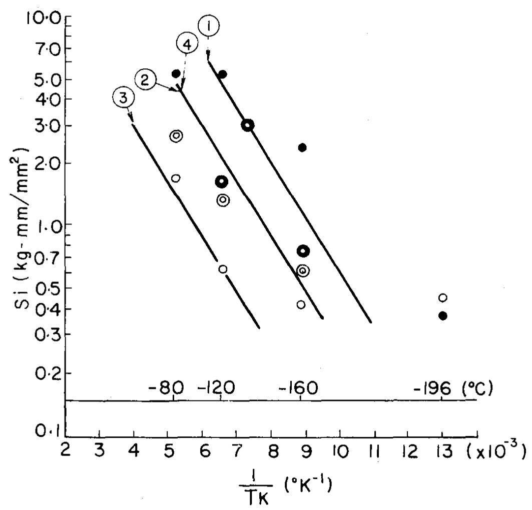


Fig. 18. Results of brittle crack initiation test (Deep-notch test, K5E, thickness; 30 mm).

| Spec. | No. | Symbol | Line-Heat Condition | Empirical Formula |
|---|---|---|---|---|
| K5D | ① | ◆ | Original Plate | $Si=193.0\cdot e^{\frac{-610.8}{T_K}}$ |
| | ② | □ | 900°C $\xrightarrow{A.C.}$ 500°C W.C. | |
| | ③ | ◇ | 800°C $\xrightarrow{A.C.}$ 700°C W.C. | $Si=31.8\cdot e^{\frac{-610.8}{T_K}}$ |
| | ④ | ◈ | 800°C $\xrightarrow{A.C.}$ 500°C W.C. | $Si=193.0\cdot e^{\frac{-610.8}{T_K}}$ |
| | ⑤ | ⟐ | 800°C A.C. | |
| | ⑥ | × | 650°C $\xrightarrow{A.C.}$ 575°C W.C. | |

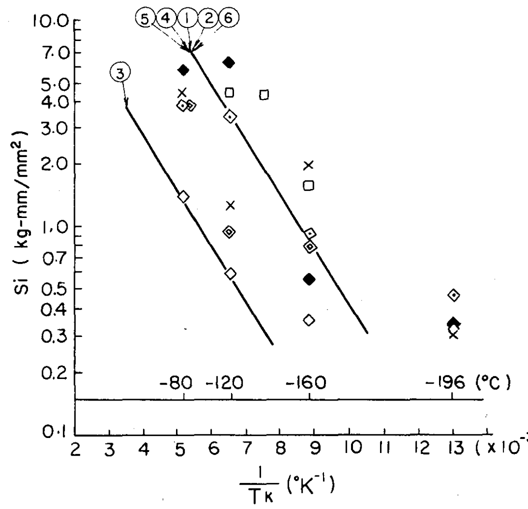


Fig. 17. Results of brittle crack initiation test (Deep-notch test, K5D, thickness; 30 mm).

| Spec. | No. | Symbol | Line-Heat Condition | Empirical Formula |
|---|---|---|---|---|
| K5D | ① | ◆ | Original Plate | $Si=44.0\cdot e^{\frac{-450.1}{T_K}}$ |
| | ② | ◇ | 800°C $\xrightarrow{A.C.}$ 500°C W.C. | |
| | ③ | ⬗ | 700°C $\xrightarrow{A.C.}$ 590°C W.C. | $Si=18.0\cdot e^{\frac{-450.1}{T_K}}$ |
| | ④ | ◈ | 700°C $\xrightarrow{A.C.}$ 500°C W.C. | $Si=44.0\cdot e^{\frac{-450.1}{T_K}}$ |
| | ⑤ | ⟐ | 700°C A.C. | |

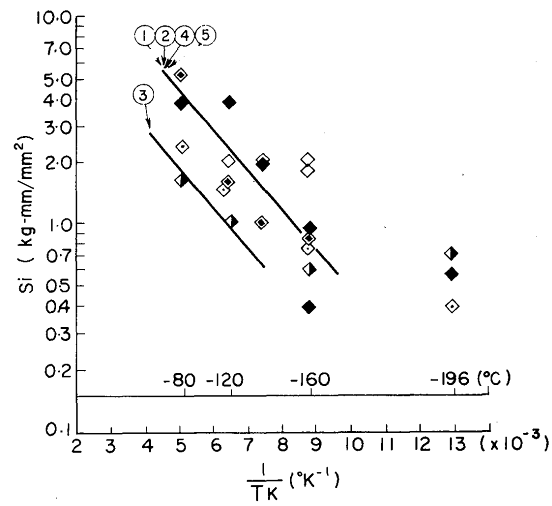


Fig. 19. Results of brittle crack initiation test (Deep-notch test, K5D, thickness; 12.7 mm).

From the results of brittle fracture initiation tests, the following can be said.

(1) The cooling methods greatly affect the brittle fracture initiation characteristics.

(2) The specimens line-heated to 700～800°C and air-cooled exhibit the brittle fracture initiation characteristics similar to those of virgin (original) steel plates from which they are taken, or a sign of slight embrittlement.

(3) The specimens line-heated to 700～900°C and water-cooled from temperatures below 500°C exhibit the brittle fracture initiation characteristics similar to those of virgin steel plates from which they are taken, or a sign of slight embrittlement.

(4) The specimens line-heated to 700～800°C and water-cooled immediately afterwards exhibit a sign of considerable embrittlement: When line-heated to below 650°C, however, the specimens exhibit no sign of such embrittlement.

### 7.3 Brittle Fracture Propagation Arrest Test

**Figures 20～23** show the results of brittle fracture propagation arrest tests on the specimens prepared as described in 6.3. The critical values of stress intensity factor $K_c$ were calculated by the following equations.

$$K_c = f(\gamma) \cdot \sigma_g \cdot \sqrt{\pi C} \quad \text{-----(8)}$$

$$\text{where } f(\gamma) = \sqrt{\frac{2}{\pi\gamma} \tan \frac{\pi\gamma}{2}} \quad \text{-----(9)}$$

$$\gamma = \frac{C}{B} \quad \text{-----(10)}$$

C = arrested crack length, mm

B = width of test specimen (direction in which the crack propagates), mm

$\sigma_g$ = gross stress, kg/mm$^2$

From the results of brittle fracture propagation arrest tests, the following can be said.

(1) For all the specimens, the brittle fracture propagation arrest characteristics vary greatly with the cooling methods adopted.

(2) When the specimens are line-heated to 700～900°C, subsequent cooling in air has only a slightly adverse effect on their brittle fracture propagation arrest characteristics while the higher the temperature from which the water-cooling is started, the less becomes the brittle fracture propagation arrest capability.

**Figure 24** shows the distribution of residual stresses at the surfaces of the 30 mm thick K5D double-tension test specimen which was line-heated to 800°C and air-cooled. Also, **Fig. 25** shows the distribution of residual stresses in the direction of plate thickness at the intermediate position on the length of the center heated line through which the crack propagates. The former figure shows the presence of considerable amounts of tensile residual stresses at the plate surfaces adjoining the center heated line, and the

| Spec. | No. | Symbol | Line-Heat Condition | Empirical Formula |
|---|---|---|---|---|
| K5A | ① | ▲ | Original Plate | $\ell n K_c = -3.46(\frac{10^3}{T_K}) + 18.28$ |
| | ② | ◭ | 900°C $\xrightarrow{A.C.}$ 625°C W.C. | $\ell n K_c = -3.46(\frac{10^3}{T_K}) + 17.39$ |
| | ③ | △ | 800°C $\xrightarrow{A.C.}$ 700°C W.C. | $\ell n K_c = -3.46(\frac{10^3}{T_K}) + 17.51$ |
| | ④ | ⟁ | 800°C $\xrightarrow{A.C.}$ 500°C W.C. | |
| | ⑤ | ◬ | 800°C A.C. | |

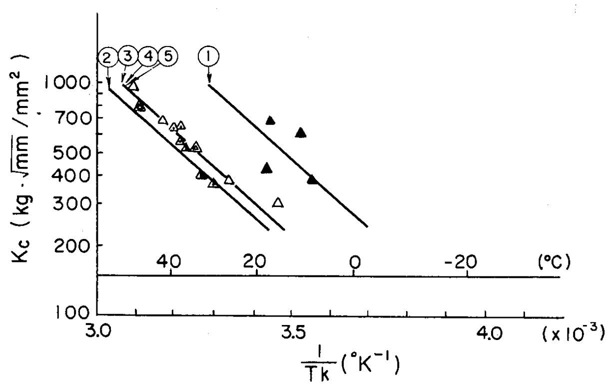


Fig. 20. Results of brittle crack propagation-arrest test (Double-tension test and ESSO test, K5A, thickness: 30 mm).

| Spec. | No. | Symbol | Line-Heat Condition | Empirical Formula |
|---|---|---|---|---|
| K5D | ① | ◆ | Original Plate | $\ell n K_c = -2.57(\frac{10^3}{T_K}) + 15.96$ |
| | ② | ⬗ | 900°C $\xrightarrow{A.C.}$ 625°C W.C. | $\ell n K_c = -2.57(\frac{10^3}{T_K}) + 15.28$ |
| | ③ | □ | 900°C $\xrightarrow{A.C.}$ 500°C W.C. | $\ell n K_c = -2.57(\frac{10^3}{T_K}) + 15.58$ |
| | ④ | ◇ | 800°C $\xrightarrow{A.C.}$ 700°C W.C. | $\ell n K_c = -2.57(\frac{10^3}{T_K}) + 15.50$ |
| | ⑤ | ◈ | 800°C $\xrightarrow{A.C.}$ 500°C W.C. | $\ell n K_c = -2.57(\frac{10^3}{T_K}) + 15.64$ |
| | ⑥ | ⟐ | 800°C A.C. | $\ell n K_c = -2.57(\frac{10^3}{T_K}) + 15.96$ |

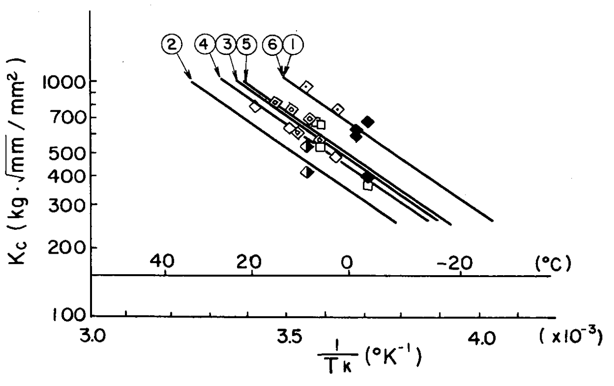


Fig. 21. Results of brittle crack propagation-arrest test (Double-tension test and ESSO test, K5D, thickness; 30 mm).

| Spec. | No. | Symbol | Line-Heat Condition | Empirical Formula |
|---|---|---|---|---|
| K5E | ① | ● | Original Plate | $\ell nKc=-2.57(\frac{10^3}{T_K})+16.03$ |
| | ② | ◑ | 900°C $\xrightarrow{A.C.}$ 625°C W.C. | $\ell nKc=-2.57(\frac{10^3}{T_K})+15.37$ |
| | ③ | **o** | 900°C $\xrightarrow{A.C.}$ 500°C W.C. | $\ell nKc=-2.57(\frac{10^3}{T_K})+15.57$ |
| | ④ | ○ | 800°C $\xrightarrow{A.C.}$ 700°C W.C. | |
| | ⑤ | ◎ | 800°C $\xrightarrow{A.C.}$ 500°C W.C. | $\ell nKc=-2.57(\frac{10^3}{T_K})+15.80$ |

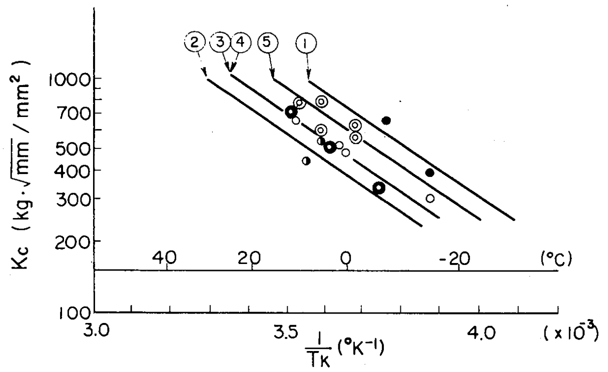


Fig. 22. Results of brittle crack propagation-arrest test (Double-tension test and ESSO test, K5E, thickness; 30 mm).

| Spec. | No. | Symbol | Line-Heat Condition | Empirical Formula |
|---|---|---|---|---|
| K5D | ① | ◆ | Original Plate | $\ell nKc=-2.05(\frac{10^3}{T_K})+14.64$ |
| | ② | half-filled ◆ | 700°C $\xrightarrow{A.C.}$ 590°C W.C. | $\ell nKc=-2.05(\frac{10^3}{T_K})+14.05$ |
| | ③ | ◇ | 700°C A.C. | $\ell nKc=-2.05(\frac{10^3}{T_K})+14.27$ |

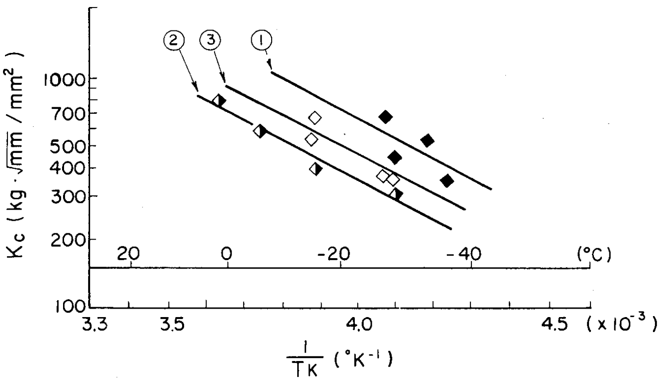


Fig. 23. Results of brittle crack propagation-arrest test (Double-tension test and ESSO test, K5D, thickness; 12.7 mm).

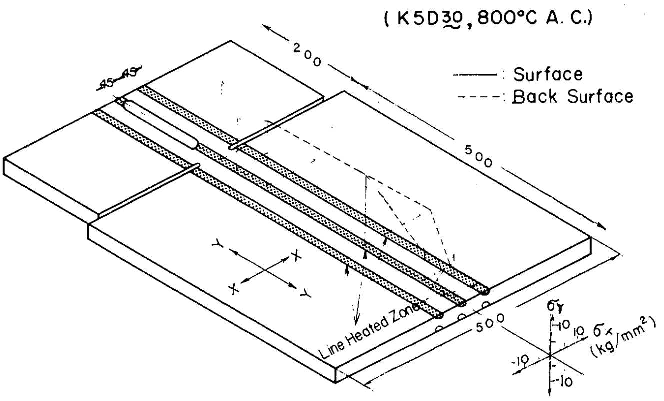


Fig. 24. Residual stress distribution of line-heated zone to 800°C and air-cooled (K5D, thickness; 30 mm).

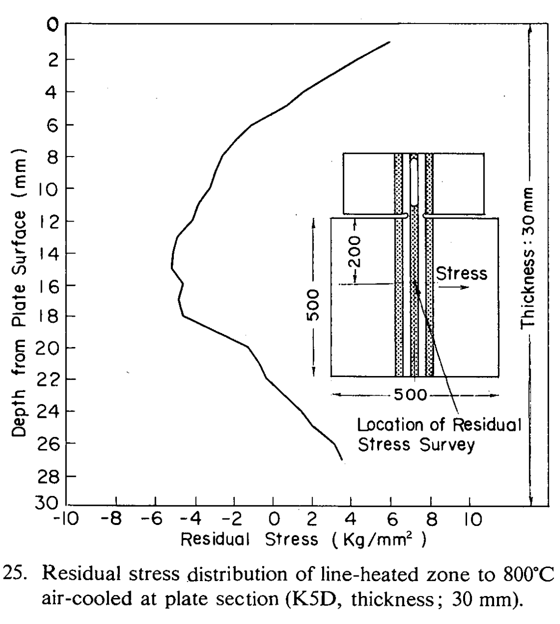


Fig. 25. Residual stress distribution of line-heated zone to 800°C and air-cooled at plate section (K5D, thickness; 30 mm).

latter figure the presence of tensile residual stresses near the plate surfaces and compressive residual stresses at the middle of plate thickness.

## 8. Considerations

### 8.1 Embrittlement Due to Line-Heating

When a steel plate is line-heated to a given maximum temperature from one side, the temperature distribution occurs across the plate thickness as shown in Fig. 5. This temperature distribution across the plate thickness takes place continuously from one torch-flame position to next in repeated thermal cycles as the line-heating progresses linearly. Exposed to the elevated temperature and then cooled with water or in air, the surface layer of the line-heated steel plate undergoes some change in microstructure and, consequently, in material properties, which in turn produces the internal strain. Thus, the line-heated steel plate becomes relatively brittle at the surface, such embrittlement being particularly pronounced when the heated surface is cooled with water.

Examination with an ordinary optical microscope of the surface layer of a steel plate line-heated to below the transformation temperature $Ac_1$ reveals no change in microstructure. The most likely explanation of the embrittlement of the surface layer heated to this temperature range will then be the quench aging or strain aging or combination of both. That is, when heated to, say, 600°C and rapidly water-cooled, carbide and nitride in the surface layer are precipitated due to supersaturation of carbon and nitrogen which normally remain dissolved in ferrite at room temperature, to result in quench aging: when heated to, say, 200~500°C, the thermal stress in the surface layer produces the internal strain and the dissolved nitrogen remains restrained in the vicinity of dislocations, to result in strain aging. Since the K5A, K5D, and K5E steels used were all aluminum-killed steels, it may be argued that most of nitrogen contained in the steels will be precipitated as the stable aluminum-nitride and no such aging phenomena will hardly occur. As can be seen from the distribution of hardnesses shown in **Fig. 26,** however, the hardness increases near a plate surface line-heated to 650°C, too, which fact attests to occurrence of the aging phenomena.

When heated to 700~800°C (immediately above the transformation temperature $Ac_1$), the microstructure in the surface layer because unstable due to partial dissolution of pearlite and, rapidly cooled with water, high-carbon martensite forms to render the surface layer substantially brittle. Distribution of hardnesses and microstructure in the surface layer heated to about 800°C and rapidly water-cooled are shown in **Figs. 26** and **27,** respectively. When cooled in air, however, the low cooling rate prevents the formation of martensite structure and produces a fine-grained bainite structure, thereby rendering the surface layer only slightly brittle.

Whether the water-cooling is provided from high

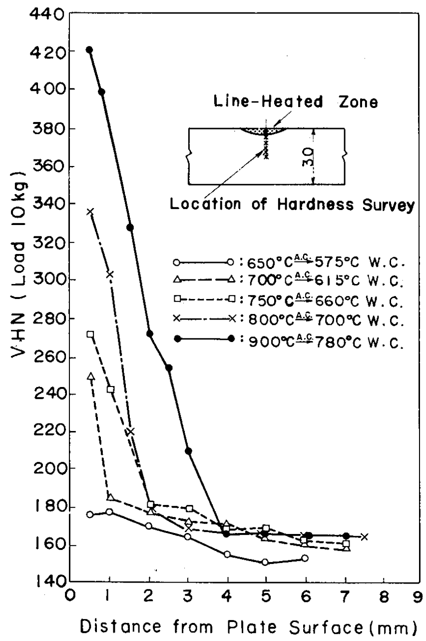


Fig. 26. Effect of maximum heating temperature on the headness of line-heated zone water-cooled just after heating (K5D).

temperatures or low temperatures makes an appreciable difference in the degree of embrittlement. For a steel plate line-heated to 800~900°C, the water-cooling from above the transformation temperature $Ar_1$ produces partial martensite structures and renders the surface layer substantially brittle in very much the same manner as if the water-cooling were provided immediately after heating. If water-cooled from below the transformation temperature $Ar_1$, however, the surface layer remains free of the martensite structure and materially as sound as if it were cooled in air.[5),6)] This phenomenon is shown in **Fig. 28** (microstructures) and **Fig. 29** (hardness).

### 8.2 Line-Heating Embrittlement of K5A, K5D, and K5E Steels

K5A, K5D, and K5E steels are embrittled differently even if they are line-heated in the same manner. It appears that K5E steel is particularly prone to embrittlement. This may be partly due to the fact that the first two steels and the last were manufactured in two different steel mills and their chemical compositions, rolling and heat-treatment conditions, etc., were not the same. It may also be mentioned that K5A steel was used as-rolled while K5D and K5E steels as-normalized.

Measurements showed that the transformation temperature $Ac_1$ of K5E steel was lower than that of K5D steel while the transformation temperature $Ar_1$ of K5E steel would shift further to the low-temperature region than that of K5D steel when water-cooled rapidly, most probably due to their differences in contents of added elements and trace elements. Therefore, since pearlite in K5E steel dissolves at the lower temperature than in K5D steel, K5E steel is affected more greatly by line-heating than K5D steel even if they are line-heated in the same manner. Also, the phase transformation in K5E steel occurs more belatedly than in K5D steel, resulting in greater quench-hardenability, and therefore, K5E steel becomes more brittle than K5D steel even if they are line-heated in the same manner.

### 8.3 Brittle Fracture Initiation and Fracture Propagation-Arrest Characteristics

**Table 3** shows for each steel plate the relation between the allowable crack length and the critical temperature for brittle fracture initiation. Values given in Table 3 were calculated using Eqs. (1)~(4) obtained from the round-bar tension test, and the equations shown in Figs. 16~19, without taking into account the effect of residual stresses which might be induced in the specimens by line-heating. The effect of such residual stresses would not be of a decisive importance

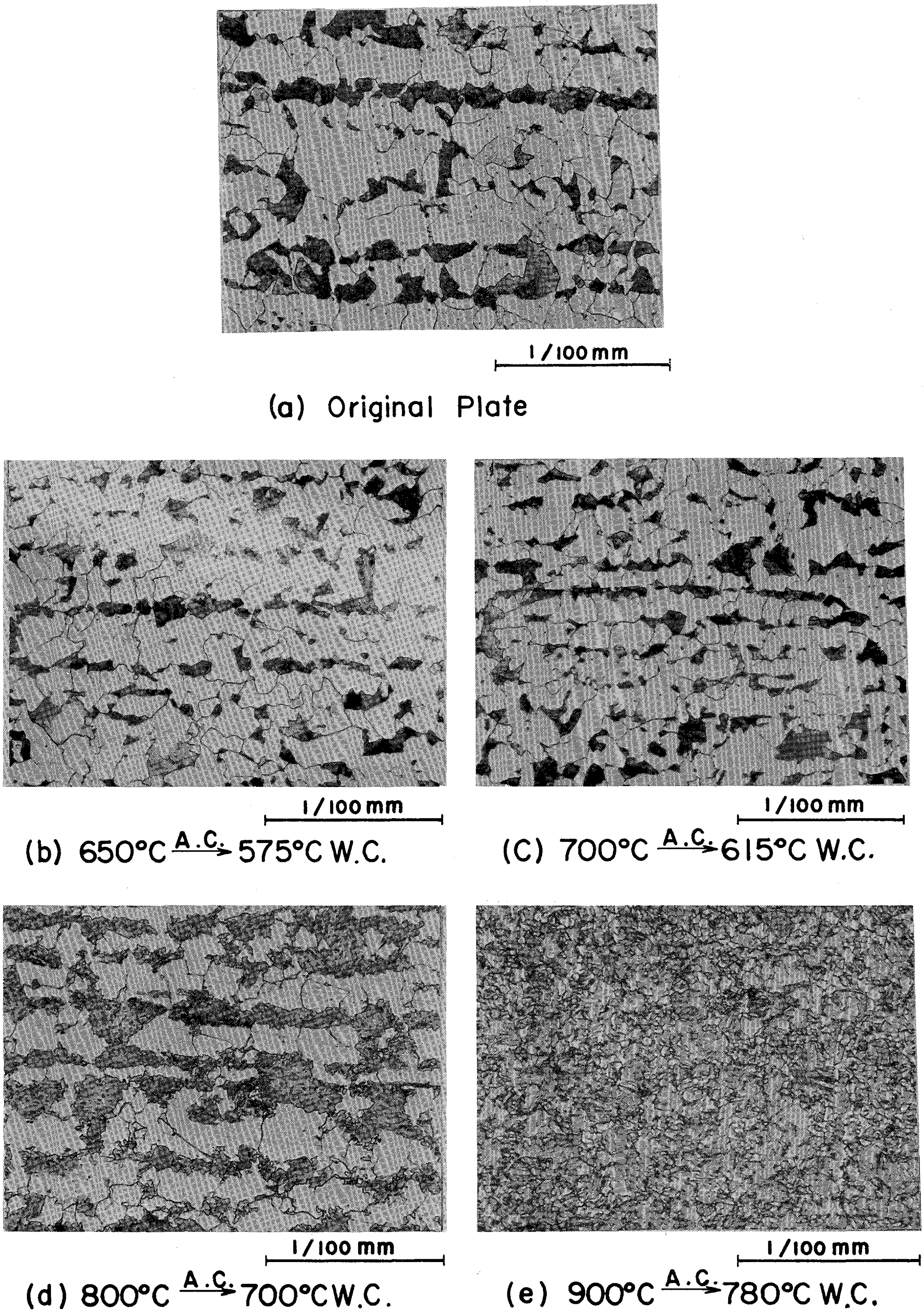


Fig. 27. Microstructures of original plate and line-heated zone (1 mm below the heated surface), heated to various maximum temperatures and water-cooled just after heating. (K5D)
(a) Original plate; (b) Maximum temperature 650°C; (c) Maximum temperature 700°C; (d) Maximum temperature 800°C; (e) Maximum temperature 900°C.

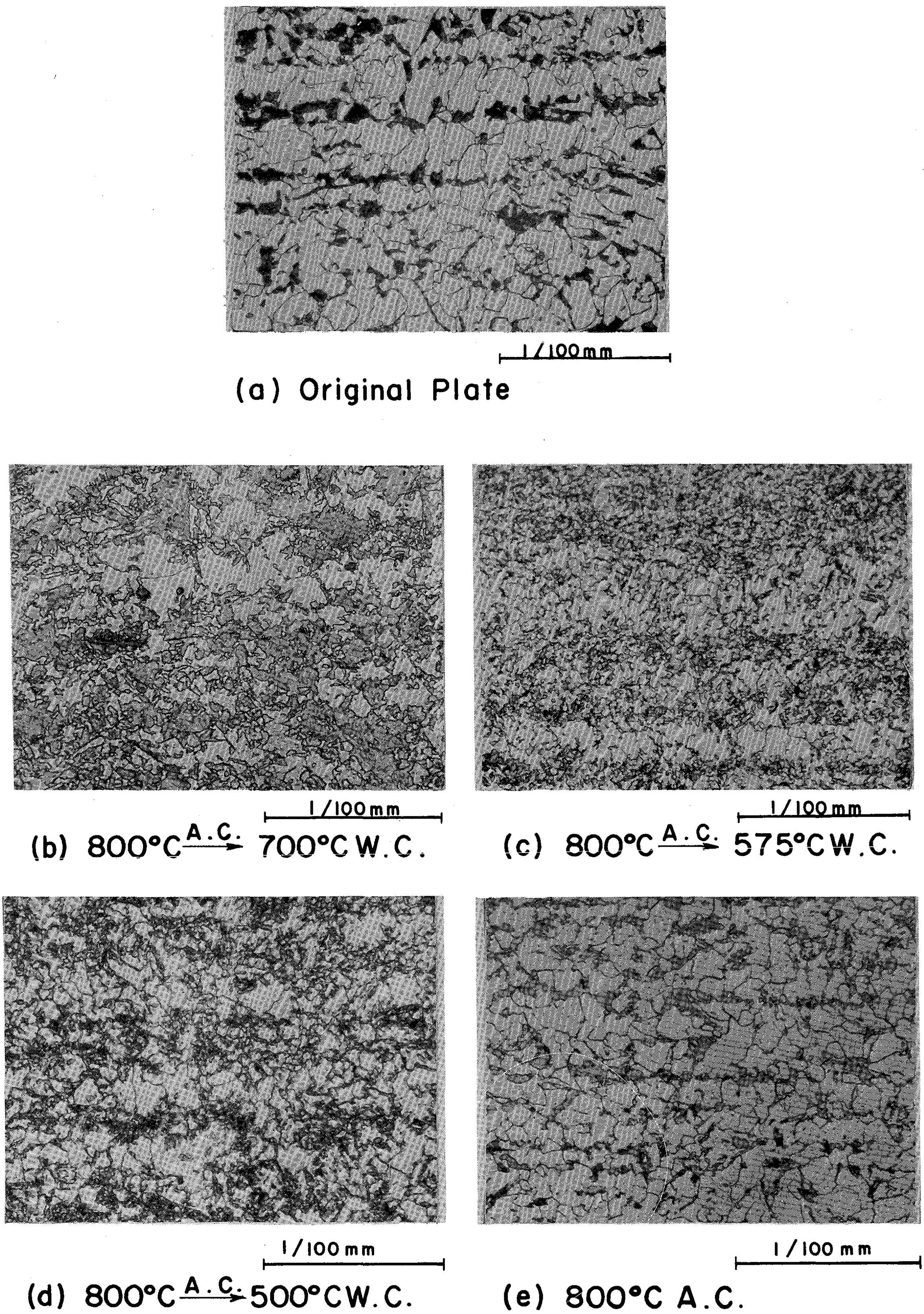


Fig. 28. Microstructures of original plate and line-heated zone (1 mm below the heated surface), heated to 800°C and water-cooled from various temperatures on cooling cycle. (K5E)
(a) Original plate; (b) Water-cooled from 700°C (just after heating); (c) Water-cooled from 575°C; (d) Water-cooled from 500°C; (e) Air-cooled to room temperature.

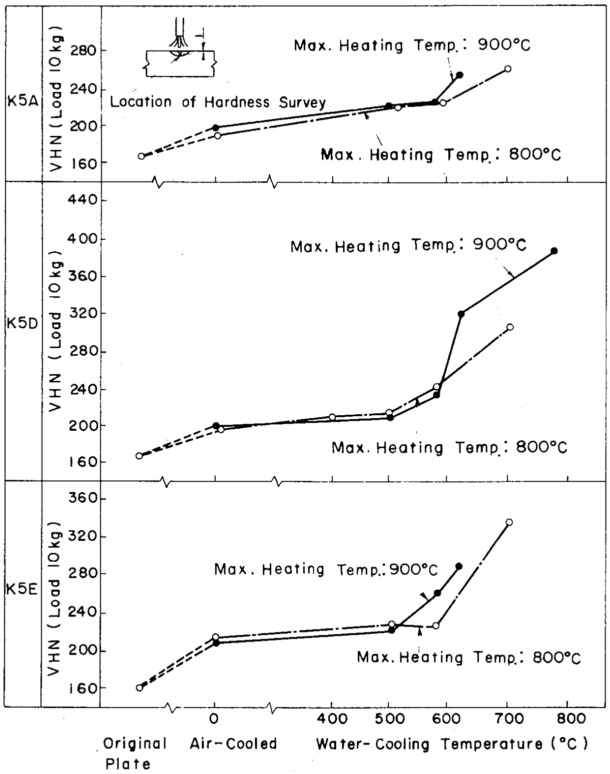


Fig. 29. Effect of water-cooling temperature on the hardness of line-heated zone.

Table 3. Critical temperature of brittle crack initiation vs. applied condition.

| Specification | Applied Stress | 16.0 kg/mm² | | | | 8.0 kg/mm² | | | | 1/2 $\sigma_y$ | | | |
|---|---|---|---|---|---|---|---|---|---|---|---|---|---|
| | Allowable Crack Length 1/2 | 100 mm | 60 mm | 30 mm | 10 mm | 100 mm | 60 mm | 30 mm | 10 mm | 100 mm | 60 mm | 30 mm | 10 mm |
| K5A (30mm thick) | Original Plate | −118°C | −136°C | −155°C | −175°C | −159°C | −169°C | −180°C | −193°C | − 92°C | −110°C | −130°C | −153°C |
| | 800°C $\xrightarrow{A.C.}$ 700°C W.C. | − 35 | − 75 | −111 | −148 | −118 | −136 | −155 | −175 | − 8 | − 46 | − 83 | −123 |
| | 800°C $\xrightarrow{A.C.}$ 500°C W.C. | − 75 | −103 | −131 | −160 | −136 | −150 | −165 | −183 | − 46 | − 75 | −104 | −136 |
| | 800°C A.C. | − 92 | −116 | −140 | −166 | −145 | −157 | −171 | −187 | − 65 | − 89 | −115 | −143 |
| K5D (30mm thick) | Original Plate<br>900°C $\xrightarrow{A.C.}$ 500°C W.C. | −141 | −154 | −168 | −185 | −171 | −179 | −188 | −199 | −105 | −121 | −139 | −161 |
| | 800°C $\xrightarrow{A.C.}$ 700°C W.C. | − 55 | − 89 | −121 | −154 | −127 | −143 | −160 | −179 | 3 | − 39 | − 80 | −121 |
| | 800°C $\xrightarrow{A.C.}$ 500°C W.C.<br>800°C A.C.<br>650°C $\xrightarrow{A.C.}$ 575°C W.C. | −141 | −154 | −168 | −185 | −171 | −179 | −188 | −199 | −105 | −121 | −139 | −161 |
| K5E (30mm thick) | Original Plate | −149 | −161 | −174 | −189 | −176 | −184 | −192 | −202 | −116 | −130 | −146 | −166 |
| | 900°C $\xrightarrow{A.C.}$ 500°C W.C. | −125 | −141 | −159 | −178 | −162 | −172 | −182 | −195 | − 86 | −106 | −128 | −152 |
| | 800°C $\xrightarrow{A.C.}$ 700°C W.C. | − 63 | − 94 | −125 | −156 | −131 | −146 | −162 | −180 | − 7 | − 46 | − 84 | −124 |
| | 800°C $\xrightarrow{A.C.}$ 500°C W.C. | −125 | −141 | −159 | −178 | −162 | −172 | −182 | −195 | − 86 | −106 | −128 | −152 |
| K5D (12.7mm thick) | Original Plate<br>800°C $\xrightarrow{A.C.}$ 500°C W.C. | −130 | −150 | −169 | −190 | −174 | −184 | −194 | −207 | −101 | −122 | −144 | −168 |
| | 700°C $\xrightarrow{A.C.}$ 590°C W.C. | − 72 | −110 | −142 | −174 | −135 | −154 | −172 | −192 | − 44 | − 80 | −115 | −149 |
| | 700°C $\xrightarrow{A.C.}$ 500°C W.C.<br>700°C A.C. | −130 | −150 | −169 | −190 | −174 | −184 | −194 | −207 | −101 | −122 | −144 | −168 |

Table 4. Critical applied temperature vs. applied condition.

| Specification | Applied Stress | 16.0 kg/mm² | | 8.0 kg/mm² | | Temperature for Required $K_c$ Value by NK Rule |
|---|---|---|---|---|---|---|
| | Allowable Crack Length | 3 m | 1 m | 3 m | 1 m | |
| K5A (30mm thick) | Original Plate | 19°C | 13°C | 3°C | − 8°C | − 5°C |
| | 900°C $\xrightarrow{A.C.}$625°C W.C. | 43 | 36 | 24 | 18 | 16 |
| | 800°C $\xrightarrow{A.C.}$700°C W.C.<br>800°C $\xrightarrow{A.C.}$500°C W.C.<br>800°C A.C. | 40 | 32 | 21 | 15 | 13 |
| K5D (30mm thick) | Original Plate | − 3 | −10 | −21 | −28 | −30 |
| | 900°C $\xrightarrow{A.C.}$625°C W.C. | 18 | 9 | − 3 | −11 | −13 |
| | 900°C $\xrightarrow{A.C.}$500°C W.C. | 8 | 0 | −12 | −18 | −21 |
| | 800°C $\xrightarrow{A.C.}$700°C W.C. | 11 | 3 | − 9 | −16 | −19 |
| | 800°C $\xrightarrow{A.C.}$500°C W.C. | 5 | − 2 | −14 | −21 | −22 |
| | 800°C A.C. | − 3 | −10 | −21 | −28 | −30 |
| K5E (30mm thick) | Original Plate | − 5 | −12 | −23 | −29 | −15 |
| | 900°C $\xrightarrow{A.C.}$625°C W.C. | 15 | 7 | − 6 | −13 | 4 |
| | 900°C $\xrightarrow{A.C.}$500°C W.C.<br>800°C $\xrightarrow{A.C.}$700°C W.C. | 9 | 1 | −11 | −18 | − 2 |
| | 800°C $\xrightarrow{A.C.}$500°C W.C. | 2 | − 6 | −17 | −24 | − 8 |
| K5D (12.7mm thick) | Original Plate | −23 | −31 | −43 | −49 | −52 |
| | 700°C $\xrightarrow{A.C.}$590°C W.C. | − 4 | −12 | −26 | −34 | −36 |
| | 700°C A.C. | −11 | −20 | −33 | −40 | −42 |

to evaluating the resistance to brittle fracture initiation for the full plate thickness under the proposed line-heating conditions.

**Table 4** shows for each steel plate the relation between the critical crack length for propagation arrest and the critical temperature. Values given in Table 4 were calculated using Eq. (8) formulated from the brittle fracture propagation resistance test, equations shown in Figs. 20~23, and the following equation which utilizes $K_c$ values for estimating the brittle fracture propagation arrest for actual structures.[7]

$$C_{eff}=0.1C+190 \quad (11)$$

where $C_{eff}$ = effective crack length determined from the results of double-tension test or ESSO test, mm

$C$ = length of brittle crack propagated in actual structures, mm

Table 4 also shows at the extreme right the temperatures which satisfy the NK-specified $K_c$ values[8] calculated from the results of brittle fracture propagation arrest test in the following manner.

K5D steel (30 mm thick): $K_c=220$ kg$\sqrt{\text{mm}}$/mm²

($\sigma$=16.0 kg/mm², C=60 mm)

K5E steel (30 mm thick): $K_c=439$ kg$\sqrt{\text{mm}}$/mm²

($\sigma$=16.0 kg/mm², C=240 mm)

For K5A steel plate and 12.7 mm thick K5D steel plate, values calculated for 30 mm thick K5D steel plate were applied.

Leaving K5A steel plate out of consideration for reason of practicality, only K5D and K5E steel plates will be studied for brittle fracture propagation arrest capability. Then, under the proposed line-heating conditions, the critical temperature is well below the lowest expected ship-plate service temperature in each instance if the applied stress is of the order of 8.0 kg/mm², which fact suggests nothing alarming about the practical use of the line-heating on these steel plates.

As mentioned earlier, the effect of residual stresses induced in the specimens by line-heating was not taken into account because the residual stresses measured in the vicinity of the path of brittle fracture propagation were tensile near the plate surface and compressive at the middle of plate thickness.

### 8.4 Evaluation of Notch Toughness

In order to determine notch toughnesses of K5A, K5D, and K5E steels, it is considered reasonable to evaluate the results of V-notch Charpy test, brittle fracture initiation test, and brittle fracture propagation arrest test in the following manner.

The 50 % crystallinity transition temperature ${}_vT_{rs}$ will be used as an acceptance criterion for evaluating the results of V-notch Charpy test.

For evaluating the results of brittle fracture initiation test, the critical temperature for brittle fracture initiation ${}_{16}T_{ic=10}$ for the applied stress of 16.0 kg/mm$^2$ (1/2×yield point at room temperature) and critical crack length of 20 mm (C=10 mm) will be used as an acceptance criterion.

For evaluating the results of brittle fracture propagation arrest test, the temperatures satisfying the NK requirements will be used as acceptance criteria: for the 30 mm-thick K5D steel, the temperature ${}_{16}T_{aK_c=220}$ for applied stress of 16.0 kg/mm$^2$ and critical crack length of 60 mm for propagation arrest, or $K_c = 220$ kg$\sqrt{mm}$/mm$^2$, and for the 30 mm-thick K5E steel, the temperature ${}_{16}T_{aK_c=439}$ for applied stress of 16.0 kg/mm$^2$ and critical crack length of 240 mm for propagation arrest, or $K_c = 439$ kg$\sqrt{mm}$/mm$^2$. For K5A steel and 12.7 mm-thick K5D steel, values calculated for the 30 mm-thick K5D steel will be used.

It is considered that for K5A, K5D, K5E, or any other similar steels, ${}_vT_{rs}$ will show a scatter of less than 20°C and ${}_{16}T_{ic=10}$, ${}_{16}T_{aK_c=220}$, and ${}_{16}T_{aK_c=439}$ a scatter of less than 10°C each as against the standard calculated value. Therefore, if each of the calculated values shifts to the high-temperature region beyond the limit of the expected scatter as a result of line-heating, then it should be interpreted that the line-heating has adversely affected the notch toughness of the steel.

${}_vT_{rs}$, ${}_{16}T_{ic=10}$, ${}_{16}T_{aK_c=220}$, and ${}_{16}T_{aK_c=439}$ calculated for each of K5A, K5D, K5E, and 12.7mm-thick K5D steel specimens are shown in **Figs. 30~33,** from which it can be said that the line-heating will exert no appreciable embrittling effect even if the steel prates are heated to above the transformation temperature $Ac_1$ (about 800~900°C), if they are cooled in air or if cooled with water from about 500°C (transformation temperature $Ar_1$) downwards, and even if they are water-cooled immediately after heating if they are heated to below the transformation temperaturet $Ac_1$ (about 600~650°C).

## 9. Conclusions

Test specimens prepared from 30 mm thick Grade A (K5A), 30 mm and 12.7 mm thick Grade D (K5D), and 30 mm thick Garde E (K5E) steel plates were line-heated with the torch flame to different temperatures up to 1000°C (measured in the plate 1 mm below the plate surface), and cooled in air or with water in different manners, for test of their notch toughness for the full plate thickness. From the test results, it can be said that the line-heating will exert no excessively embrittling effect if it is carried out in the following manner.

(1) The steel plate may be heated to 800~900°C provided it is cooled in air afterwards.
(2) The steel plate may be heated to 600~650°C if it is cooled with water immediately afterwards.
(3) The steel plate may be heated to 800~900°C if it is water-cooled after being cooled in air to below 500°C.

It is, therefore, quite possible to apply the line-heating for the 50 kg/mm$^2$-class high-tensile steel plates more efficiently, without adversely affecting their notch toughness, by choosing proper medium and timing for cooling.

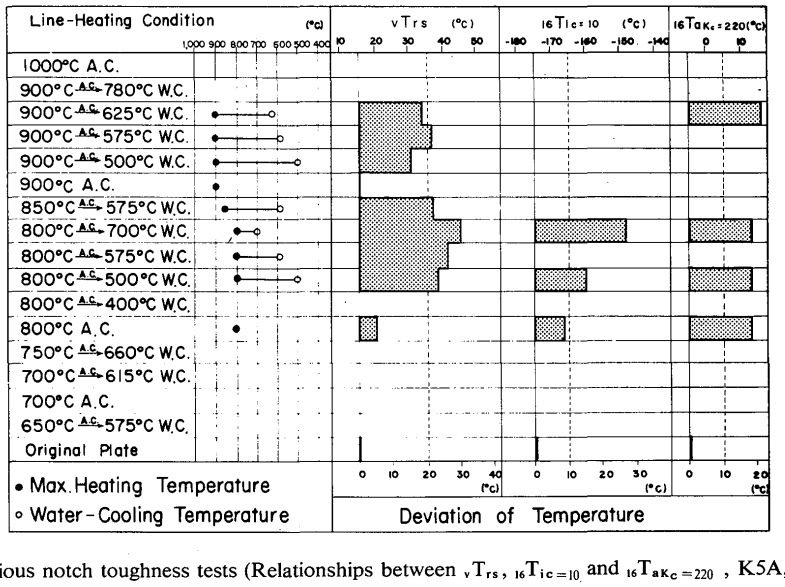


Fig. 30. Results of various notch toughness tests (Relationships between ${}_vT_{rs}$, ${}_{16}T_{ic=10}$ and ${}_{16}T_{aK_c=220}$, K5A, thickness; 30 mm).

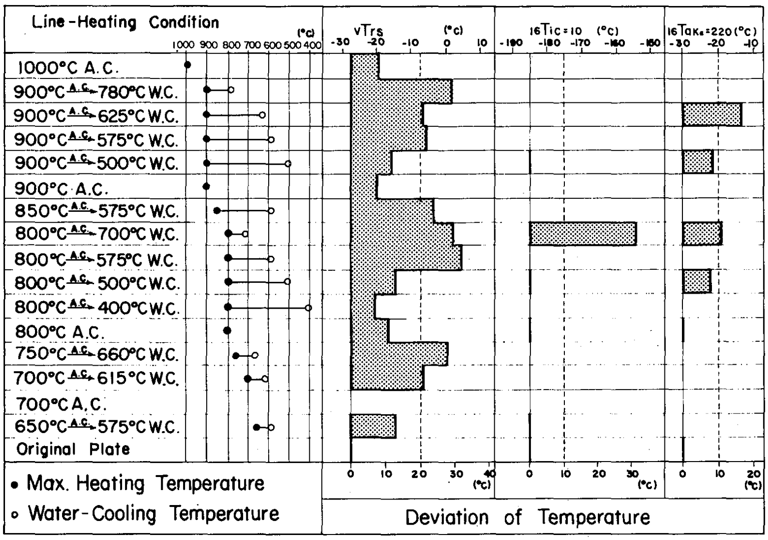


Fig. 31. Results of various notch toughness tests (Relationships between ${}_{v}T_{rs}$, ${}_{16}T_{ic=10}$ and ${}_{16}T_{aK_c=220}$, K5D, thickness; 30 mm).

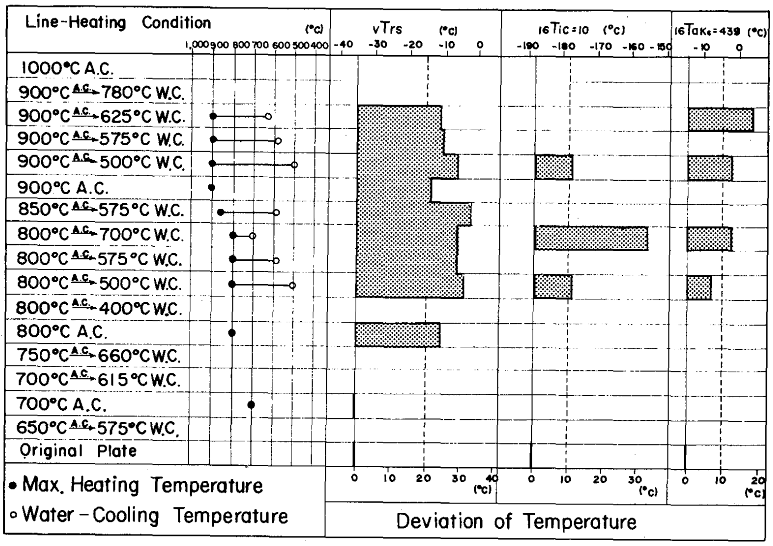


Fig. 32. Results of various notch toughness tests (Relationships between ${}_{v}T_{rs}$, ${}_{16}T_{ic=10}$, ${}_{16}T_{aK'_c=439}$, K5E, thickness; 30 mm).

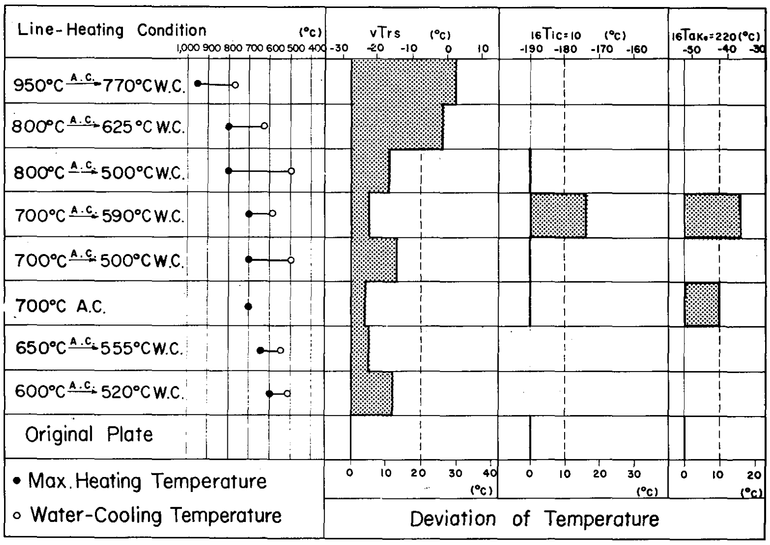


Fig. 33. Results of various notch toughness tests (Relationships between ${}_{v}T_{rs}$, ${}_{16}T_{ic=10}$ and ${}_{16}T_{aK_c=220}$, K5D, thickness; 12.7 mm).

## Acknowledgement

This project was suggested by the Shipbuilding Process Research Committee of The Society of Naval Architects of Japan and conducted by the 111 Research Committee of The Japan Shipbuilding Research Association to which the authors belong. The authors wish to express their heartfelt thanks to the members of both committees for fruitful discussions and cooperations, and also to the technical staffs of the Department of Structural Engineering, Nagasaki University and The Nagasaki Technical Institute of Mitsubishi Heavy Industries, Ltd., who kindly assisted the authors for carrying out the various test.


### References


1) Shipbuilding Department of Ishikawajima-Harima Heavy Industries: "Bending Process of Line-Heated Plates", Ishikawajima Eng. Rev. Vol. 11, No. 35: Vol. 13, No. 40 and No. 41.
2) H. Kihara and K. Ikeda. "On Brittle Fracture Initiation (Second Report)— Brittle Fracture Initiation Characteristics—", J. Soc. Naval Arch. Japan, Vol. 118, 1965.
3) M. Yoshiki, T. Kanazawa and S. Machida: "A Consideration on Brittle Fracture Test of Steel Plates—with Special Reference to Flat-Temperature and Gradient Temperature Type Double Tension Test—" J. Soc. Naval Arch. Japan, Vol. 113, 1963.
4) Y. Akita and K. Ikeda: "On the Propagation and Arrest of Brittle Crack, with Special Reference to ESSO Test with Temperature Gradient", J. Soc. Naval Arch. Japan, Vol. 112, 1962.
5) H. Suzuki, H. Tamura, Y. Kawano and T. Hashiguchi: "Me llurgical Study of Heat-Affected Zone in Steels by Welding Heat Cycle Reappearing System (Report No. 3)", Journal of Japan Welding Society, Vol. 27, No. 5, 1958.
6) M. Inagaki, K. Nakahara, K. Harada and Y. Mitani: "Notch Toughness in Welding Heat Reappearing Structure Around Bond Zones of High Tensile Strength Steels of Various Types", Journal of Japan Welding Society, Vol. 33, No. 9, 1964.
7) H. Kihara, T. Kanazawa, K. Ikeda, H. Maenaka, M. Kinoshita, R. Nagamoto and H. Yajima: "Effectiveness of Crack Arrester (2nd Report)", J. Soc. Naval Arch. Japan, Vol. 124, 1968.
8) Nippon Kaiji Kyokai, Hull Department: "Standard for Impact Tests of High-Strength Steels for Hull Plates and Classification of Application to Hull Construction", Regulation of Nippon Kaiji Kyokai, 1965.